

Quantum neural networks with multi-qubit potentials

Yue Ban,^{1,2} E. Torrontegui,^{3,4} and J. Casanova^{1,5}

¹*Department of Physical Chemistry, University of the Basque Country UPV/EHU, Apartado 644, 48080 Bilbao, Spain*

²*School of Materials Science and Engineering, Shanghai University, 200444 Shanghai, People's Republic of China*

³*Departamento de Física, Universidad Carlos III de Madrid, Avda. de la Universidad 30, 28911 Leganés, Spain*

⁴*Instituto de Física Fundamental IFF-CSIC, Calle Serrano 113b, 28006 Madrid, Spain*

⁵*IKERBASQUE, Basque Foundation for Science, Euskadi Plaza 5, 48009, Bilbao, Spain*

We propose quantum neural networks that include multi-qubit interactions in the neural potential leading to a reduction of the network depth without losing approximative power. We show that the presence of multi-qubit potentials in the quantum perceptrons enables more efficient information processing tasks such as XOR gate implementation and prime numbers search, while it also provides a depth reduction to construct distinct entangling quantum gates like CNOT, Toffoli, and Fredkin. This simplification in the network architecture paves the way to address the connectivity challenge to scale up a quantum neural network while facilitates its training.

I. INTRODUCTION

Information has become a resource due to its advance and expansion in the digitalization and control [1]. However, programming explicit algorithms with good performance may become unfeasible due to the vertiginous growth in (i) the amount of available information with which classical algorithms have to deal [2], and (ii) the inherent difficulty of finding efficient algorithms for specific problems [3]. All this limits our current capabilities in information processing tasks. Two alternative approaches that would contest these limitations are machine learning and quantum computing [4, 5].

On the one hand, machine learning (ML) is a branch of artificial intelligence that uses statistical techniques to give computers the ability to progressively learn with input data without being explicitly programmed. ML is based on the generation of a hypothesis that is optimized from sample inputs and re-used to generate new predictions [6]. Thus the algorithms can learn from data and overcome the static program instructions by making data-driven decisions from sample inputs. Among the distinct hypothesis models, neural networks [7] are very extended due to the blooming of deep learning [8, 9]. Similar to biological networks, artificial neural networks are organized in layers and each layer learns new behavior patterns [10]. The computational power of artificial neural networks relies on this architecture where *neurons* in each layer feed signals into other neurons allowing parallel-processed computing [11, 12]. In this manner, several calculations can be performed at the same time, and large computational problems can often be divided into smaller ones, which can be then solved simultaneously. The versatility of neural networks to classify complex data relies on the *universal approximation theorem*, which leads artificial neural networks the capacity to approximate any function [13]. As result, they span a broad range of applications such as speech [14] or object recognition [15], spam filters [16], vehicle control [17, 18], trajectory prediction [19], decision making [20], game-playing [21], or automated trading systems [22].

On the other hand, quantum computing represents a different paradigm from classical information processing. Based on

an alternative information encoding that exploits the quantum properties of matter, systems that encompass several quantum bits (qubits) are exponentially hard to simulate with classical devices [5] showing that quantum systems do not seem to obey Church thesis [23], and consequently they are not polynomially equivalent to classical systems. Then, quantum systems harnessed as computational devices, might be dramatically more powerful than any other classical system [24]. The universality of quantum computing [25] expands a broad range of applications. Some examples are linear systems solvers [26], molecule simulators [27], combinatorial optimizers [28], black-box [29] and factorization problems [30], or Hamiltonian simulations [31]. Although a set of single $N = 1$ and two-qubit $N = 2$ gates is a universal approximator [32], larger multi-qubit ($N > 2$) gates may offer a computational advantage that reduces complexity in existing algorithms [33–35].

Quantum machine learning [36–44] aims for the symbiosis of both paradigms to the mutual reinforcement. The use of quantum resources allows improvements of the machine learning protocol accuracy in classification and regression tasks compared to their classical counterparts [46–50]. On the other hand, the universality of artificial networks may enhance the accuracy and efficiency of quantum protocols [45, 51–54].

In this work, we propose an extension of a universal quantum neural network (QNN) [44] enabling multi-qubit ($N > 2$) interactions that lead to an enhancement of the approximation power, and a reduction of the network depth. As result, achieving a simplification of existing protocols not only requires shorter operation times, but it may also introduce less accumulation of errors due to the reduction in the amount of requested gates. The paper is structured as follows: We firstly introduce the quantum perceptron model under the presence of multi-qubit interactions. We define the quantum perceptron as a single-output quantum neuron connected to several-input quantum neurons without hidden layers. The result of nesting several quantum perceptrons is a QNN. We show that a quantum perceptron with multi-qubit interactions can do an XOR gate and prime number search from 3 to 5 bits, improving the performance of approximation power compared to the classical counterpart, as well as with standard QNNs

(i.e. QNNs that include several nested perceptrons without multi-qubit interactions). Then, we show that quantum gates such as CNOT, Toffoli, and Fredkin can be implemented by QNN involving quantum perceptrons with multi-qubit interactions, thus reducing the circuit depth as it is not needed to add hidden layers.

II. QUANTUM PERCEPTRONS WITH MULTI-QUBIT POTENTIALS

A quantum perceptron, or quantum neuron, is the basic building block of a QNN. It can be constructed as a qubit that presents a nonlinear response to an input potential \hat{x}_j in the excitation probability. This can be written as the following quantum gate acting on a j th qubit that encodes the quantum perceptron [44, 45]:

$$\hat{U}_j(\hat{x}_j; f)|0_j\rangle = \sqrt{1 - f(\hat{x}_j)}|0_j\rangle + \sqrt{f(\hat{x}_j)}|1_j\rangle. \quad (1)$$

The transformation in Eq. (1) can be engineered by evolving adiabatically the qubit with, for instance, the Hamiltonian

$$\hat{H} = \frac{1}{2} [\hat{x}_j \hat{\sigma}_j^z + \Omega(t) \hat{\sigma}_j^x] \quad (2)$$

where \hat{x}_j is the potential exerted by other neurons on the perceptron, and the applied external field $\Omega(t)$ leads to a tunable energy gap in the dressed-state qubit basis $|\pm\rangle$, with $\hat{\sigma}_j^x |\pm\rangle = \pm |\pm\rangle$. Typically, $\hat{x}_j = \sum_{i=1}^k (w_{ji} \hat{\sigma}_i^z) - b_j$ [44, 45] which implies that the j th perceptron is coupled to a number k of neurons (labelled with i) in the previous/input layer via standard spin-spin interactions. The Hamiltonian in Eq. (2) has the following reduced eigenstate (i.e. when the degrees of freedom of any other neuron are traced-out):

$$|\Phi(x_j/\Omega(t))\rangle = \sqrt{1 - f(x_j/\Omega(t))}|0_j\rangle + \sqrt{f(x_j/\Omega(t))}|1_j\rangle, \quad (3)$$

where $f(x)$ corresponds to a sigmoid excitation probability

$$f(x) = \frac{1}{2} \left(1 + \frac{x}{\sqrt{1 + x^2}} \right). \quad (4)$$

Specifically, to accomplish $\hat{U}_j(\hat{x}_j; f)|0_j\rangle$, one can use a Hadamard gate to firstly get the transformation $|0_j\rangle \rightarrow |+\rangle$ and finally obtain $|\Psi\rangle = |\Phi(x_j/\Omega(t_f))\rangle$ at a certain time t_f by evolving the system adiabatically with Hamiltonian (2). In this manner, the non-linear activation function of the quantum perceptron is encoded in the probability of the excited state $P_j = f(\hat{x}_j) = \frac{1}{2}(1 + \langle \hat{\sigma}_j^z \rangle)$ during the adiabatic evolution [44]. In order to speed up the operation of this perceptron, one can also use inverse engineering techniques which directly impose conditions in the wave function evolution at the initial and final time instants, resulting in a smooth control $\Omega(t)$ [45]. In addition, this accelerated activation mechanism for the quantum neurons would reduce the decoherence in the system leading to enhanced performance.

Now, we introduce a different type of potentials which rely on the possibility to implement multi-qubit interactions. In particular, we consider a potential of the kind

$$\hat{x}_j = \sum_{i=1}^k (w_{ji} \hat{\sigma}_i^z) + w_m \hat{\sigma}_{l_1}^z \dots \hat{\sigma}_{l_n}^z - b_j. \quad (5)$$

where w_m is a multi-qubit coefficient marked by the subscript m , and $l_p \in [1, 2, \dots, k]$ (namely, the term involving several Pauli matrices includes products of an arbitrary number of neurons in the previous input). For the sake of simplicity in the presentation, there is only a single multi-qubit term in Eq. (5). However, this can include several products of distinct neurons in the input layer (i.e. additional multi-qubit terms). Later we will provide examples of these of interactions each of them associated to a specific problem.

The Hamiltonian given by Eqs. (2) and (5) corresponds to the linear Ising Hamiltonian with higher order interactions. Such a model is present in distinct quantum platforms [56–58]. Interestingly, quantum evolutions governed by terms involving up to six-qubit interactions has already been implemented in trapped-ion systems [59]. Each of the next examples considered below correspond to a particular case of multi-qubit interaction and its physical implementation would depend on the specific considered platform.

In the following, we show that multi-qubit potentials enable tasks such as (i) constructing XOR gates at the perceptron level (ii) searching prime numbers and (iii) encoding quantum gates. All these are implemented without hidden layers and/or ancillary qubits, thus, showing the significant role of multi-qubit potentials in the simplification of QNNs.

A. XOR gate

As a classical perceptron is a linear separator, a non-linear logic gate such as the well-known XOR problem (i.e., the exclusive OR boolean function) requires at least one hidden layer to be implemented in classical neural networks [60]. Now we show that a quantum perceptron with multi-qubit interactions in the neural potential is a non-linear classifier. In particular, we illustrate the construction of an XOR gate by a single quantum perceptron with multi-qubit interactions. We also show that the lack of hidden layers prevents classical neural network and standard QNN to achieve the same task.

As the values of the output neuron 0 and 1 cannot be separated linearly, a classical perceptron with two inputs and one output (i.e. without hidden layers) fails to solve the XOR gate. To show this, we use the standard gradient descent algorithm to train this simple classical perceptron with a sigmoidal activation potential $f(x)$, see Eq. (4), and $x_j = \sum_{i=1}^k w_{ij} s_i - b_j$ with the classical input $s_j \in \{0, 1\}$ whose cost function is in the form of the mean square value

$$C = \frac{1}{2N} \sum_{n=1}^N (y^{(n)} - t^{(n)})^2. \quad (6)$$

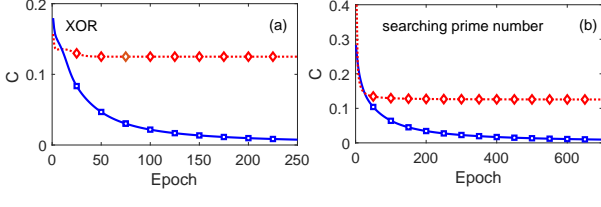


FIG. 1. In order to (a) encode an XOR gate and to (b) search prime numbers among the integers from 0 to 7, we show the value of the cost function at different epoches, using a multi-qubit interaction perceptron (solid blue) and a classical perceptron (dotted red). The latter is equivalent to a quantum perceptron with only two-qubit terms, which is shown from the comparison of the weights and bias during the training process, see Eqs. (7, 8, 9), where the learning rate is $\eta = 1.5$. The transfer function in Eq. (4) is used for both cases. In the quantum perceptron, this function indicates the system evolves adiabatically.

Here, $N = 4$ determines the four possible examples 00, 10, 01, 11, while $y^{(n)}$ and $t^{(n)}$ are the output and the target respectively, for the n th example. During the training, the parameters of the classical perceptron are updated after each epoch as

$$\begin{aligned}\tilde{w}_i &= w_i - \eta \frac{\partial C}{\partial w_i} = w_i - \frac{\eta}{N} \sum_{n=1}^N (y^{(n)} - t^{(n)}) f'(x) s_j, \\ \tilde{b} &= b - \eta \frac{\partial C}{\partial b} = b - \frac{\eta}{N} \sum_{i=1}^N (y^{(n)} - t^{(n)}) f'(x),\end{aligned}\quad (7)$$

with the learning rate η . Any other sigmoid-like function $g(x)$, similar to $f(x)$, can be applied to train this perceptron in order to obtain the same approximation power. As it is shown in Fig. 1 (a), the cost function value of this classical perceptron stuck in $C = 0.125$ (dotted-red line with superimposed diamonds for a better identification). Thus, a classical perceptron can only converge on linearly separable data, i.e. it is not able to imitate the XOR function. In order to complete an XOR, a hidden layer with two neurons is needed. These two neurons can be regarded to perform an OR and a NAND gate.

To implement an XOR gate with a quantum perceptron without the multi-qubit term in Eq. (5), this is by using the potential $\hat{x} = w_1 \hat{\sigma}_1^z + w_2 \hat{\sigma}_2^z - b$, one can follow the procedure described in Ref. [44]. To encode an XOR gate, the neural potential is derived from the four basis states $|00\rangle, |01\rangle, |10\rangle, |11\rangle$, which play the role of the four examples of the input in the XOR gate (namely, 00, 10, 01, 11). In this case, as the input values of the XOR gate are bits, one can transform them into the measurement value of $\hat{\sigma}^z$ of the input qubits for the perceptron, i.e. $\sigma_{\text{in}}^z = \frac{1}{2}(1 + \langle \hat{\sigma}^z \rangle)$. Therefore, the input values 0 and 1 refer to the input states as the ground state $|0\rangle$ ($\langle \hat{\sigma}^z \rangle = -1$) and the excited state $|1\rangle$ ($\langle \hat{\sigma}^z \rangle = 1$), respectively.

Such a quantum perceptron without hidden layers and with only two-qubit interactions is equivalent to a classical perceptron, from the point of view of the following training process. Aiming at training it with the gradient descent method, one

has to update the weights and bias as

$$\begin{aligned}\tilde{w}_i &= w_i - \frac{\eta}{N} \sum_{n=1}^N (y^{(n)} - t^{(n)}) \frac{\partial C}{\partial x} \frac{\partial x}{\partial w_i}, \\ \tilde{b} &= b - \frac{\eta}{N} \sum_{i=1}^N (y^{(n)} - t^{(n)}) \frac{\partial C}{\partial x},\end{aligned}\quad (8)$$

where

$$\frac{\partial C}{\partial x} = \frac{1}{2} \left(\left\langle \frac{\partial \Psi}{\partial x} | \hat{\sigma}_z | \Psi \right\rangle + \left\langle \Psi | \hat{\sigma}_z | \frac{\partial \Psi}{\partial x} \right\rangle \right) = f'(x) \quad (9)$$

and $|\Psi\rangle = \hat{U}(x, f)|0\rangle$ is the solution to the Schrödinger equation driven by the Hamiltonian (2) with $\hat{x} = w_1 \hat{\sigma}_1^z + w_2 \hat{\sigma}_2^z - b$. In the previous equations we can see that weights and bias are obtained in the same way as their classical counterparts. For that, one has to compare Eq. (7) with Eqs. (8) and (9) provided that $\frac{\partial x}{\partial w_i} = \hat{\sigma}_j^z \rightarrow s_j$. This indicates that a single quantum perceptron with two-qubit interactions and the basis states $|00\rangle, |01\rangle, |10\rangle, |11\rangle$ as input is equivalent to a classical perceptron.

In order to implement the XOR gate with this quantum perceptron, one would need to perform two adiabatic passages with different controls $\Omega(t)$, as well as to use different neural potentials in each passage by appropriately changing the weights and biases [44]. Equivalently, one could also do the XOR gate by including one hidden layer with two additional quantum neurons and the application of a single $\Omega(t)$. It is worth mentioning that Eq. (9) holds only for a quantum perceptron instead of a QNN with hidden layers. If a QNN has more layers, one only needs to measure the output qubit value $P(x_j) = \frac{1}{2}(1 + \langle \Psi | \hat{\sigma}_j^z | \Psi \rangle)$ instead of the intermediate ones, i.e., $|\Psi\rangle = \hat{U}_{\text{tot}}|0\rangle$ with $\hat{U}_{\text{tot}} = \prod_{j=1}^M \hat{U}_j$ where M is the total number of quantum perceptrons in QNN. Otherwise, shot noise is introduced by measuring the neurons in the hidden layer.

This procedure to do the XOR gate can be simplified when considering a quantum perceptron with multi-qubit interactions. In particular, we explore the following multi-qubit potential

$$\hat{x} = w_1 \hat{\sigma}_1^z + w_2 \hat{\sigma}_2^z - b + w_m \hat{\sigma}_1^z \hat{\sigma}_2^z. \quad (10)$$

For simplicity, the subscript j labelling the perceptron is neglected, as we are working with a single quantum perceptron. In this case, the weights w_1, w_2 and b are updated as in Eqs. (8), while the updating formula for the weight of the $w_m \hat{\sigma}_1^z \hat{\sigma}_2^z$ term is

$$\tilde{w}_m = w_m - \frac{\eta}{N} \sum_{n=1}^N (y^{(n)} - t^{(n)}) \frac{\partial C}{\partial x} \hat{\sigma}_1^z \hat{\sigma}_2^z. \quad (11)$$

The existence of $w_m \hat{\sigma}_1^z \hat{\sigma}_2^z$ in the neural potential enables the quantum perceptron to construct an XOR gate as a non-linear separator. To prove this point, we test the cost function value (see, Eq. (6)) for our quantum perceptron and find that $C < 1\%$ occurs at epoch = 197 as shown in Fig. 1 (a) (solid-blue line with squares). On the contrary the classical and qubit-qubit interaction perceptron are not able to produce an XOR gate, see plateau behavior of the cost function (dotted-red) that remains constant after the epoch ~ 50 .

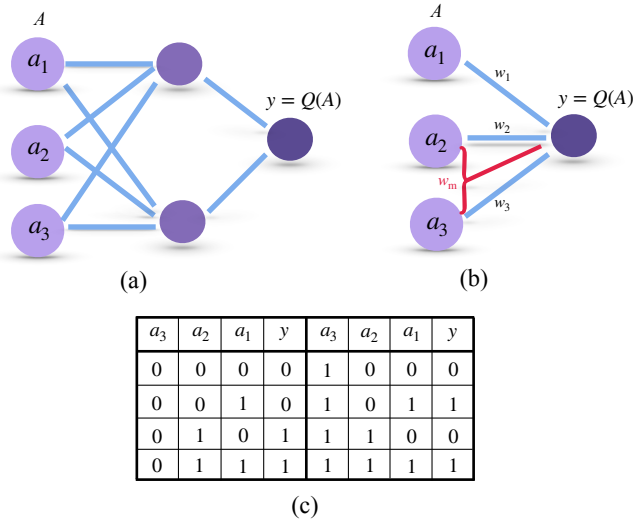


FIG. 2. (a) Schematic configuration of a classical neural network with one hidden layer of two neurons for the task to search prime numbers of the input number $A = (a_1, a_2, a_3) \in \{0, 1, \dots, 7\}$ with 3 bits. After well trained, the network gives the output $y = Q(A)$. (b) The same task can be achieved by a QNN which has multi-qubit interactions in the neural potential (red junction involving second and third neurons) without hidden layers. (c) Truth table for prime-number search with 3 input bits for a QNN. The input values $A = (a_1, a_2, a_3)$ are the binary numbers for the integers from 0 to 7. The output value $y = Q(A)$ is 1 for prime numbers and 0 for non-prime ones.

B. Searching prime numbers

In Ref. [44], a specific example of two, three, and four perceptrons per layer was illustrated to detect prime numbers from 0 to $2^i - 1$ where i ranges from $i = 3$ to $i = 7$ bits. In particular, it was shown that a QNN with two perceptrons –one in the hidden layer and the other one as the output– can classify prime numbers from 0 to 7 (3 bits). This exemplifies the better performance of QNNs compared with classical ones where a hidden layer with two neurons are necessary to accomplish the same task. A scheme of these networks is shown figure in Fig. 2 (a) and (b), while details regarding QNN-training to search prime numbers are in Appendix A.

Now, we introduce the multi-qubit term into the neural potential and find that the same task is achieved by a QNN without hidden layers, i.e. at the single quantum perceptron level. To search a prime number for 3 bits (Truth table listed in Fig. 2 (c)) using a single quantum perceptron we consider the potential

$$\hat{x} = w_1 \hat{\sigma}_1^z + w_2 \hat{\sigma}_2^z + w_3 \hat{\sigma}_3^z - b + w_m \hat{\sigma}_2^z \hat{\sigma}_3^z. \quad (12)$$

As we demonstrate later, adding the multi-qubit term $w_m \hat{\sigma}_2^z \hat{\sigma}_3^z$ is enough to fulfill the prime numbers searching task. In this respect, one can include additional multi-qubit terms in the neural potential. However, we use the simplest example in Eq. (12) to simplify the network and training process.

We note that when the input of a quantum perceptron that presents only two-qubit interactions are the basis states, this is equivalent to the classical perceptron as shown in Eqs. (7, 8, 9). For this reason, now we compare the cost function of a classical perceptron with the cost function of a quantum perceptron using the potential in Eq. (12) for the specific purpose of searching prime numbers from 0 to 7. As it is shown in Fig. 1 (b) the quantum perceptron achieves $C < 1\%$ at epoch= 667 (solid-blue with squares), while the C value saturates to 0.126 in the classical counterpart (dotted-red with diamonds). This indicates that our perceptron achieves the searching task without hidden layers. We have also verified the ability of the quantum perceptron by minimizing the cost function to an acceptable error for searching prime numbers for 4 bits with the potential

$$\hat{x} = w_1 \hat{\sigma}_1^z + w_2 \hat{\sigma}_2^z + w_3 \hat{\sigma}_3^z + w_4 \hat{\sigma}_4^z - b + w_m \hat{\sigma}_2^z \hat{\sigma}_3^z, \quad (13)$$

and for 5 bits with

$$\begin{aligned} \hat{x} = & w_1 \hat{\sigma}_1^z + w_2 \hat{\sigma}_2^z + w_3 \hat{\sigma}_3^z + w_4 \hat{\sigma}_4^z + w_5 \hat{\sigma}_5^z - b \\ & + w_m \hat{\sigma}_2^z \hat{\sigma}_3^z. \end{aligned} \quad (14)$$

The multi-qubit terms in the above two neural potentials for 4 and 5 bits are chosen due to the fact that the cost function result in $C < 1\%$ at epoch = 1692 for Eq. (13) and epoch = 1698 for Eq. (14) with the consideration of adopting the minimal number of multi-qubit terms. Further training the above quantum perceptrons presents that the value of C tends to 0 asymptotically, proving the success to achieve these tasks.

C. Quantum gates

Now we show that one can use a QNN with multi-qubit interactions to construct quantum gates such as CNOT gate, Toffoli, and Fredkin without the necessity of hidden layers. In comparison, one can demonstrate that a QNN with only two-qubit interactions cannot construct the above mentioned quantum gates in the same conditions. This will be shown later. As quantum gates are reversible, the number of input and output qubits of quantum gates should be equal. Hence, the number of the neurons in the input equals that in the output. Correspondingly, the cost function is changed into

$$C = \frac{1}{2Nk} \sum_{n=1}^N \sum_{i=1}^k (y_i^{(n)} - t_i^{(n)})^2, \quad (15)$$

where k is the number of quantum perceptrons.

For CNOT gate where $k = 2$, the truth table and the schematic configuration of the QNN is shown in Fig. 3 (a) and (b) respectively, where each perceptron (output neuron) gives the output value $y_i = \frac{1}{2}(1 + \langle \hat{\sigma}_{\text{out},i}^z \rangle)$. The first perceptron should have the same value as the first input neuron, while the second one aims to achieve the same value as the XOR output of two input neurons, i.e. $\hat{\sigma}_{\text{out},2}^z = \hat{\sigma}_1^z \oplus \hat{\sigma}_2^z$ [61]. The neural potential of the second perceptron is

$$\hat{x}_2 = w_{21} \hat{\sigma}_1^z + w_{22} \hat{\sigma}_2^z - b + w_m \hat{\sigma}_1^z \hat{\sigma}_2^z, \quad (16)$$

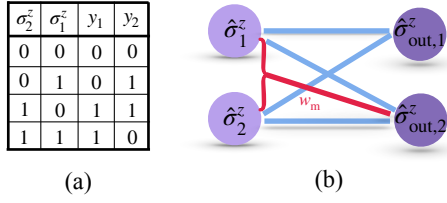


FIG. 3. Truth table of a CNOT gate (a) constructed by a QNN illustrated in a schematic configuration (b) with the multi-qubit interaction term $w_m \hat{\sigma}_1^z \hat{\sigma}_2^z$.

and the first perceptron has two-qubit interaction terms. We find that this is the most concise choice, as it requires least connectivity. We obtain the cost function value (using Eq. (15)) $C < 1\%$ at epoch = 116 and $C \rightarrow 0$ at a larger epoch, as shown in Fig. 4 (a) (solid-blue with squares) indicating the satisfaction to train a CNOT gate well. On the contrary, training such a CNOT gate by a QNN with only two-qubit interaction terms leads to a C tending to 0.0625 at large epoch, see Fig. 4 (b). This indicates that a standard QNN cannot encode the CNOT without hidden layers.

A QNN with multi-qubit terms also works for constructing a Toffoli gate without hidden layers. Truth table, and QNN for Toffoli are shown in Fig. 5 (a) and (b). Known as Controlled-Controlled-Not gate, a Toffoli gate has 3-qubit inputs and outputs. In the QNN, the outputs of the first two qubits should be the same value as their inputs $\hat{\sigma}_{\text{out},i}^z = \hat{\sigma}_i^z$ ($i = 1, 2$), while the output of the third qubit aims at $\hat{\sigma}_{\text{out},3}^z = \hat{\sigma}_3^z \oplus \hat{\sigma}_1^z \hat{\sigma}_2^z$ [61]. In this case, we propose the following neural potential of the third perceptron

$$\hat{x}_3 = w_{31} \hat{\sigma}_1^z + w_{32} \hat{\sigma}_2^z + w_{33} \hat{\sigma}_3^z - b + w_m \hat{\sigma}_1^z \hat{\sigma}_2^z \hat{\sigma}_3^z, \quad (17)$$

with a minimal number of multi-qubit terms. Demonstrated in Fig. 4 (a) and (b), the value $C < 1\%$ (dashed-red line with

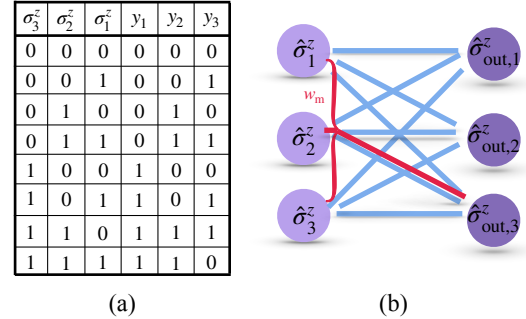


FIG. 5. Truth table of a Toffoli gate (a) constructed by a QNN illustrated in a schematic configuration (b) with the multi-qubit interaction term $w_m \hat{\sigma}_1^z \hat{\sigma}_2^z \hat{\sigma}_3^z$.

crosses) occurs at epoch = 140 and goes to 0 at large epoch during the training of a Toffoli gate. In close similarity with the previous case, a standard QNN without hidden layers fails to achieve the Toffoli gate, as C saturates at 0.0238.

Another example that can be successfully constructed by our QNNs including multi-qubit interactions without hidden layers is the Fredkin gate (also known as Controlled-SWAP gate) whose truth table and schematic configuration are in Fig. 6 (a) and (b). In this case, the adopted potential of the third perceptron is

$$\hat{x}_3 = w_{31} \hat{\sigma}_1^z + w_{32} \hat{\sigma}_2^z + w_{33} \hat{\sigma}_3^z - b + w_m \hat{\sigma}_1^z \hat{\sigma}_2^z \hat{\sigma}_3^z, \quad (18)$$

The cost function value C tends to zero asymptotically, shown in Fig. 4 (a) (dotted-black line with asterisks), indicating that these gates can be constructed by quantum perceptrons without hidden layers. Again, C saturates at the value 0.0417 at large epoch for a standard QNN without hidden layers, see Fig. 4 (b).

III. DISCUSSION

We have shown different application of QNNs which possess multi-qubit interactions. These terms induce connectivities among quantum perceptrons that deviate from the current network paradigm of additive activations. It is due to the multi-qubit terms in the potentials that one can avoid the presence of internal hidden layers without sacrificing approximative power. Meanwhile, the performance is enhanced compared to the same topology of a QNN without multi-qubit interactions. Such architecture allows us to address the connectivity challenge in scaling up QNNs. Moreover, the simple configuration helps to control the efficiency of the training processes. During the training process of all the examples shown above, the activation function (Eq. 4) based on the adiabatic evolution of the system is used. Instead, one may use *shortcuts to adiabaticity* to accelerate the formation of the activation function in physical registers [45].

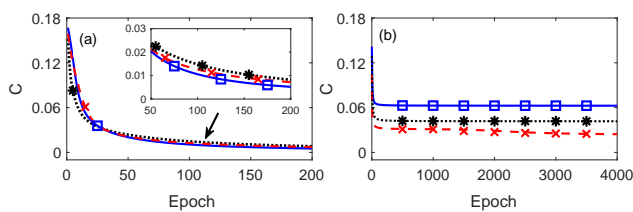


FIG. 4. Cost function at different epoch for (a) QNN with the multi-qubit term and (b) QNN with only two-qubit interactions. In particular the solid-blue line is the cost function obtained to construct a CNOT gate, a Toffoli gate (dashed-red line) and a Fredkin gate (dotted-black line). Illustrated in the inset of (a), the cost function values reach $C < 1\%$ at 116th, 140th, 162th epoch for the above three quantum gates, respectively, indicating that these gates can be constructed by QNNs with multi-qubit interaction without hidden layers. In contrast, C values go to their respective plateau by quantum perceptrons with two-qubit interactions.

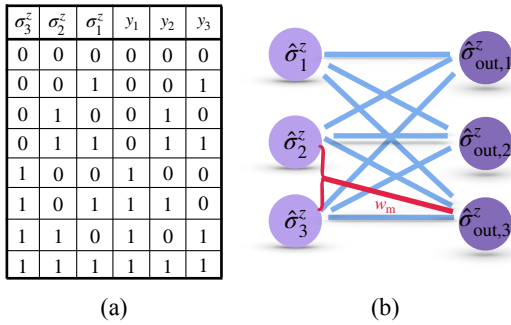


FIG. 6. Truth table of a Fredkin gate (a) constructed by a QNN illustrated in a schematic configuration (b) with the multi-qubit interaction term $w_m \hat{\sigma}_2^z \hat{\sigma}_3^z$.

IV. CONCLUSION

We propose a QNN with multi-qubit interactions included in the potential. We show that this QNN can perform distinct tasks without hidden layers. Among them we can list XOR gate encoding, searching prime number (in our case from 3 to 5 bits) as well as to construct quantum gates such as the CNOT, Toffoli, and Fredkin gates at the perceptron level. The reduction in the topologies of the networks not only simplifies the training process but also improve the accuracy of the approximation. The usage of less quantum perceptrons in the network can increase the process fidelity due to less decoherence effects when the QNN is encoded in physical registers.

ACKNOWLEDGEMENTS

We acknowledge financial support from Spanish Government via PGC2018-095113-B-I00 (MCIU/AEI/FEDER, UE), Basque Government via IT986-16, as well as from QMiCS (820505) and OpenSuperQ (820363) of the EU Flagship on Quantum Technologies, and the EU FET Open Grant Quromorphic (828826). C.M.-J. acknowledges the predoctoral MICINN grant PRE2019-088519. E. T. acknowledges financial support from Project PGC2018-094792-B-I00 (MCIU/AEI/FEDER, UE), CSIC Research Platform PTI-001, CAM/FEDER Project No. S2018/TCS-4342 (QUITEMAD-CM), and by Comunidad de Madrid-EPUC3M14. J. C. acknowledges the Ramón y Cajal program (RYC2018-025197-I) and the EUR2020-112117 project of the Spanish MICINN, as well as support from the UPV/EHU through the grant EHUrOPE.

Appendix A: Training for prime numbers search

To train a QNN for the task of searching prime numbers, a set of 2^i pairs for i bits containing the input and output values $\{A^{(n)}, y^{(n)}\}_{n=1}^{2^i}$ is taken, where the inputs are binary numbers

$A^{(n)} = (a_1, a_2, \dots, a_i)$ corresponding to the integers belonging to the set $\in \{0, 1, \dots, 2^i - 1\}$. As the targets are $t \in \{0, 1\}$, the output of the network $y^n = Q(A^{(n)}) = 1$, if and only if the input number is prime.

- [1] M. Castells, *The Information Age: Economy, Society and Culture*, Blackwell, Oxford, 1996.
- [2] C. Walter, *Scientific American* **293**, 32 (2005).
- [3] A. Kolmogorov, *Sankhya Ser. A* **25**, 369 (1963).
- [4] A. L. Samuel, *IBM Journal of Research and Development* **3**, 210 (1959).
- [5] R. P. Feynman, *Int. J. Theor. Phys.* **21**, 467 (1982).
- [6] D. Hebb, *The Organization of Behavior*, Wiley, New York, 1949.
- [7] W. S. McCulloch and W. Pitts W, *Bull. Math. Biol.* **5**, 115 (1943).
- [8] K.-Su Oh and K. Jung, *Pattern Recognition* **37**, 1311 (2004).
- [9] Y. LeCun, Y. Bengio, and G. Hinton, *Nature* **521**, 436 (2015).
- [10] S. C. Kleene, *Representation of Events in Nerve Nets and Finite Automata*, *Annals of Mathematics Studies* **34**, Princeton University Press (1956).
- [11] F. Rosenblatt, *The perceptron - A perceiving and recognizing automaton*, Tech. Rep. 85-460-1, Cornell Aeronautical Laboratory, (1957).
- [12] J. J. Hopfield, *Proc. Nat. Acad. Sci.* **81**, 3088 (1984).
- [13] G. Cybenko, *Math. Control Signals Syst.* **2**, 303 (1989).
- [14] G. E. Dahl, D. Yu, L. Deng, and A. Acero, *IEEE Transactions on Audio, Speech and Language Processing*, **20**, 33 (2012).
- [15] G. E. Hinton, S. Osindero, and Y. Teh, *Neural Comput.* **18**, 1527 (2006).
- [16] E. G. Dada, J. S. Bassi, H. Chiroma, S. M. Abdulhamid, A. O. Adetunmbi, and O. E. Ajibawa, *Helijon* **5**, e01802 (2019).
- [17] M. Buehler, K. Iagnemma, and S. Singh, *The DARPA urban-challenge: autonomous vehicles in city traffic*, Springer, vol. 56, 2009.
- [18] S. Devi, P. Malarvezhi, R. Dayana and K. Vadivukkarasi, *Wirel. Pers. Commun.* **114**, 2121 (2020).
- [19] A. Valsamis and K. Tserpes, D. Zisis and D. Anagnostopoulos, and T. Varvarigou, *J. Syst. Softw.*, **127** 249, (2017).
- [20] P. Kashyap, *Machine Learning for Decision Makers: Cognitive Computing Fundamentals for Better Decision Making*, APress, U. S. (2018).
- [21] J. Fürnkranz, *Machine Learning and Game Playing, Encyclopedia of Machine Learning*, Springer US, 2010.
- [22] B. Huang, Y. Huan, L. D. Xu, L. Zheng, and Z. Zou, *Enterp. Inf. Syst.* **13**, 132 (2019).
- [23] S. C. Kleene, *Duke Math. J.* **2**, 340 (1936).
- [24] F. Arute, K. Arya, R. Babbush, et al., *Nature* **574**, 505 (2019).
- [25] A. Y. Kitaev, *Russ. Math. Surv.* **52**, 1191 (1997).
- [26] A. W. Harrow, A. Hassidim, and S. Lloyd, *Phys. Rev. Lett.* **103**, 150502 (2009).
- [27] A. Peruzzo, J. McClean, P. Shadbolt, M. Yung, X. Zhou, P. J. Love, A. Aspuru-Guzik, and J. L. O'Brien, *Nat. commun.* **5**, 4213 (2014).
- [28] E. Farhi, J. Goldstone, and S. Gutmann, *arXiv:1411.4028* (2014).
- [29] L. K. Grover, A fast quantum mechanical algorithm for database search, *Proceedings, 28th Annual ACM Symposium on the Theory of Computing*, 1996, p. 212.

[30] P. W. Shor, Algorithms for quantum computation: discrete logarithms and factoring, *Proceedings 35th Annual Symposium on Foundations of Computer Science*, 1994, p. 124.

[31] S. Lloyd, Universal quantum simulators, *Science* **273**, 1073 (1996).

[32] M.A. Nielsen and I. Chuang, *Quantum Computation and Quantum Information*, Cambridge University Press, New York, U. S. (2011).

[33] Mikko Möttönen, J. J. Vartiainen, V. Bergholm, and M. M. Salomaa, *Phys. Rev. Lett.* **93**, 130502 (2004).

[34] M. Reagor, C. B. Osborn, N. Tezak, et al., *Sci. Adv.* **8**, eaao3603 (2018).

[35] T. Bækkegaard, L. B. Kristensen, N. J. S. Loft, C. K. Andersen, D. Petrosyan, and N. T. Zinner, *Sci. Rep.* **9**, 13389 (2019).

[36] S. C. Kak, *Adv. Imag. Elect. Phys.* **94**, 259 (1995).

[37] M. Schuld, I. Sinaysky, and F. Petruccione, *Quan. Info. Proc.* **13**, 2567 (2014).

[38] J. Biamonte, P. Wittek, N. Pancotti, P. Rebentrost, N. Wiebe, and S. Lloyd, *Nature* **549**, 195 (2017).

[39] E. Farhi and H. Neven, arXiv:1802.06002 (2018).

[40] M. Schuld and N. Killoran, *Phys. Rev. Lett.* **122** 040504 (2019).

[41] M. Schuld, A. Bocharov, K. Svore, and N. Wiebe, *Phys. Rev. A* **101**, 032308 (2020).

[42] Y. Cao, G. Guerreschi, A. Aspuru-Guzik, arXiv: 1711.11240 (2017).

[43] A. Pérez-Salinas, A. Cervera-Lierta, E. Gil-Fuster, and J. I. Latorre, *Quantum* **4**, 226 (2020).

[44] E. Torrontegui and J. J. García-Ripoll, *Europhys. Letts.* **125**, 30004 (2019).

[45] Y. Ban, X. Chen, E. Torrontegui, E. Solano and J. Casanova, *Sci. Rep.* **11**, 5783 (2021).

[46] S. Gupta and R. K. P. Zia, *J. Comput. Syst. Sci.* **63**, 355 (2001).

[47] G. D. Paparo, V. Dunjko, A. Makmal, M. A. Martin-Delgado, and H. J. Briegel, *Phys. Rev. X* **4**, 031002 (2014).

[48] M. Benedetti, J. Realpe-Gómez, R. Biswas, and A. Perdomo-Ortiz, *Alejandro*, *Phys. Rev. X* **7**, 041052 (2017).

[49] G. Sentís, M. Guta, and G. Adesso, *EPJ Quantum Technol.* **2**, 17 (2015).

[50] V. Havlíček, A. D. Corcónes, K. Temme, A. W. Harrow, A. Kandala, J. M. Chow, and J. M. Gambetta, *Nature* **567**, 209 (2019).

[51] J. Carrasquilla and R. G. Melko, *Nat. Phys.* **13**, 431 (2017).

[52] D.- L. Deng, X. Li, and S. Das Sarma, *Phys. Rev. X* **7**, 021021 (2017).

[53] G. Torlai, G. Mazzola, J. Carrasquilla, M. Troyer, R. Melko, and G. Carleo, *Nat. Phys.* **14**, 447 (2018).

[54] N. Aharon, A. Rotem, L. P. McGuinness, F. Jelezko, A. Retzker, and Z. Ringel, *Sci. Rep.* **9**, 17802 (2019).

[55] Y. Ban, J. Echanobe, Y. Ding, R. Puebla, J. Casanova, arXiv: 2012.07677 (2020).

[56] I. S. Donskaya, *Theor. Math. Phys.* **74**, 324 (1988).

[57] S. Kumar. H. Zhang, and Y. P. Huang, *Commun. Phys.* **3**, 108 (2020).

[58] M. Sameti, A. Potočnik, D. E. Browne, A. Wallraff, and M. J. Hartmann, *Phys. Rev. A* **95**, 042330 (2017).

[59] B. P. Lanyon, C. Hempel, D. Nigg, M. Müller, R. Gerritsma, F. Zähringer, P. Schindler, J. T. Barreiro, M. Rambach, G. Kirchmair, M. Hennrich, P. Zoller, R. Blatt, and C. F. Roos, *Science* **334**, 57 (2011).

[60] M. Minsky and S. A. Papert, *Perceptrons: An Introduction to Computational Geometry*, Cambridge, MA, USA: MIT Press, 2017.

[61] M. A. Nielsen and I. L. Chuang, *Quantum Computation and Quantum Information*, Cambridge university press, 2010.